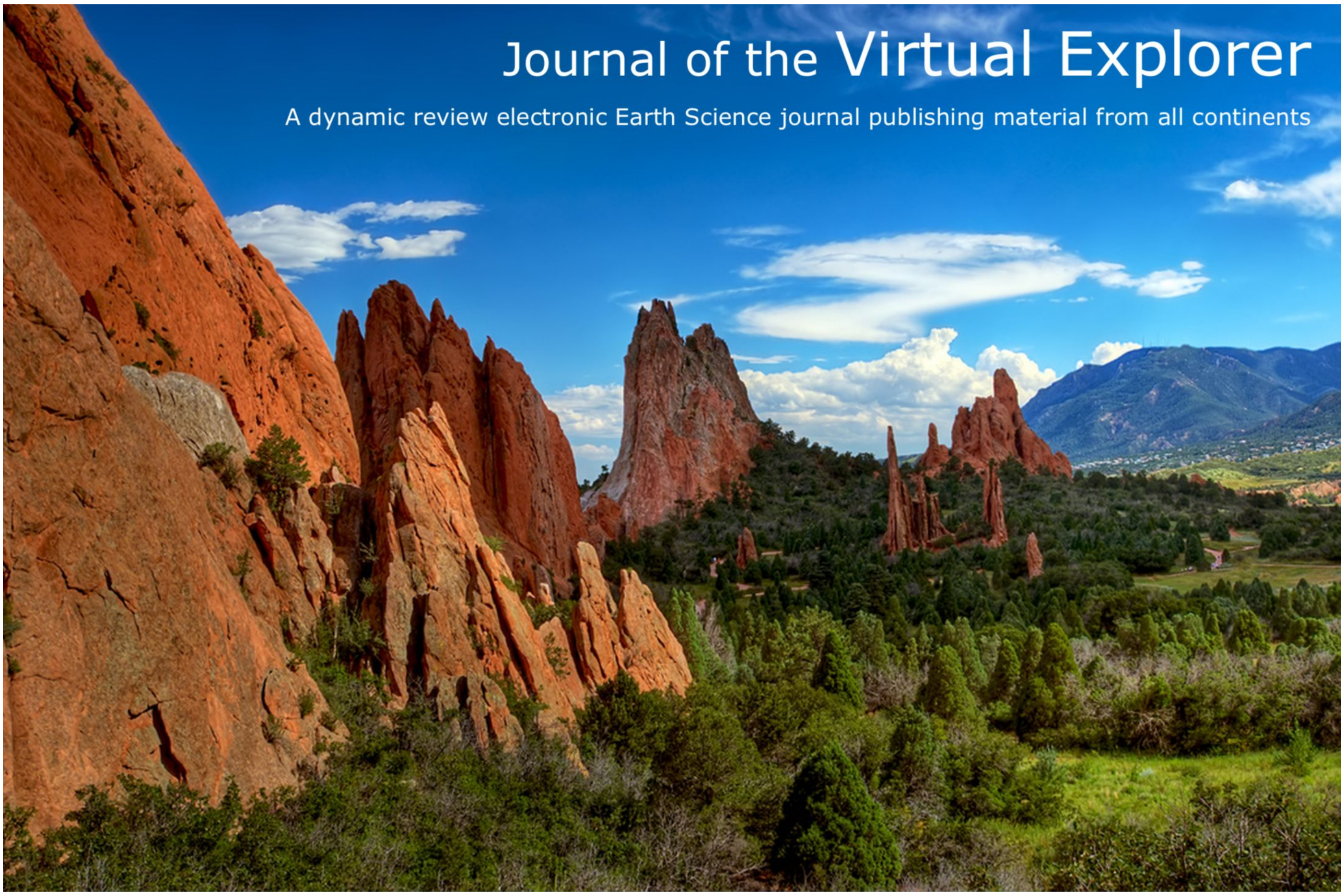

Structure and metamorphism of Amorgos: a field excursion

Gideon Rosenbaum, Uwe Ring

Journal of the Virtual Explorer, Electronic Edition, ISSN 1441-8142, volume **27**, paper 7
In: (Eds.) Gordon S. Lister, M.A. Forster, and Uwe Ring,
Inside the Aegean Metamorphic Core Complexes, 2007.

Structure and metamorphism of Amorgos: a field excursion

Gideon Rosenbaum

Earth Sciences, University of Queensland, Brisbane QLD 4072, Australia. *Email: g.rosenbaum@uq.edu.au*

Uwe Ring

Department of Geological Sciences, University of Canterbury, Christchurch 8140, New Zealand.

Abstract: This field excursion focuses on structural and metamorphic aspects in the island of Amorgos, which is normally considered to represent the stratigraphy of external units in the Hellenides. The excursion includes two itineraries. The first one is in the area northwest of Katapola, where two distinct high-pressure units are exposed. High-pressure mineral assemblages include (1) blue amphibole, garnet and clinopyroxene; and (2) Fe-Mg-carpholite, quartz, phengite and paragonite. The contact between the two units is a low angle detachment fault. The second itinerary starts in the famous monastery of Hozoviotíssas and ends in the northern port of Egiali. The excursion passes through some good examples of folding and provides constraints on the multiple-phase deformation history of the island.

Citation: 2007. Structure and metamorphism of Amorgos: a field excursion. In: (Eds.) Gordon S. Lister, M.A. Forster, and Uwe Ring, *Journal of the Virtual Explorer*, volume **27**, paper 7, doi: 10.3809/jvirtex.2007.00181

Introduction

The island of Amorgos is located approximately 35 km east of Naxos in the central Aegean Sea (Figure 1). It separates the Cycladic Blueschist Unit (Dürr *et al.*, 1978; Bonneau, 1984) from rocks of the Lycian Nappes farther east (De Graciansky, 1972; Bernoulli *et al.*, 1974), and can therefore provide important information on the regional correlations of orogenic components (Jolivet *et al.*, 2004).

The geology of Amorgos has been mapped by Dürr (1985) and was the topic of relatively few published articles (Renz, 1933; Tataris, 1965; Dürr *et al.*, 1978; Minoux *et al.*, 1980; Fytrolakis *et al.*, 1981). Most of these studies concentrated on lithological aspects, mostly suggesting that the stratigraphy of Amorgos resembles the stratigraphy of the Tripoliza zone of the external Hellenides. In addition, there are a number of studies dealing with the neotectonics of Amorgos (Papadopoulos and Pavlides, 1992; Stiros *et al.*, 1994; Perissoratis and Papadopoulos, 1999), particularly because of the destructive 1956 MS = 7.4 earthquake, which occurred southeast of Amorgos and generated a tsunami with waves reaching a height of 20-30 m in the southern coast of the island.

The structure and metamorphism of Amorgos have so far received relatively little attention (Theye *et al.*, 1997). Some new information has been provided in our recent study (Rosenbaum *et al.*, 2007), but there are still many open questions and uncertainties.

In this field excursion we provide a general introduction to the structure and metamorphism of Amorgos. The excursion can be done in 2 days

Figure 1. Amorgos

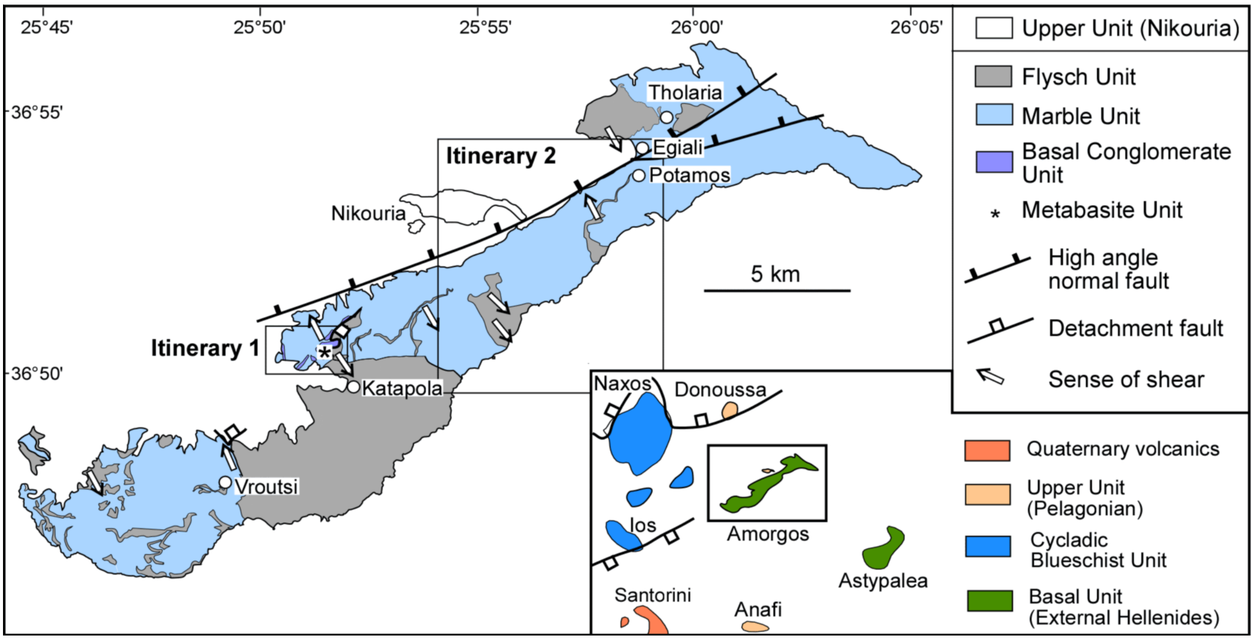

Simplified geological map of Amorgos (modified after Dürr, 1985) showing the locations of the two itineraries.

Geological setting

Rocks in Amorgos have been sub-divided into the following tectonostratigraphic units (Rosenbaum *et al.*, 2007): the Metabasite Unit, the Basal Conglomerate Unit, the Marble Unit, and the Flysch Unit.

The two lowermost units are found only in the area northwest of Katapola (Itinerary 1). They consist of two distinct blueschist-facies assemblages associated with (1) garnet/blue-amphibole metabasites, and (2) carpholite-bearing micaschists, quartzites and meta-conglomerates.

Overlying these units is a thick (>1000 m) Triassic to Eocene marble sequence. This includes, from bottom to top, massive marbles, meta-dolomites, well bedded pelagic marbles with abundant meta-chert replacements, and thick massive marbles with a few small lenses of Cretaceous meta-bauxites (Dürr *et al.*, 1978; Fytrolakis *et al.*, 1981; Dürr, 1985). The meta-bauxites can be found in the northern part of the island, where they contain the assemblage diaspore, hematite and Fe-carpholite (Minoux *et al.*, 1980), estimated by Theye *et al.* (1997) to represent metamorphic conditions of 300-400°C and >8 kbar.

The top of the stratigraphic sequence in Amorgos is made up of a Flysch unit, which consists of shales, schists, greywackes, conglomerates and large marble olistoliths. The flysch conglomerates are characterised by centimetre- to decimetre-scale pebbles of marbles and greywackes, shales, schists and quartzites.

The structural history of Amorgos involved at least three phases of deformation (Rosenbaum *et al.*, 2007). The earliest one is associated with isoclinal recumbent folds (F1) and is responsible for the development of the dominant penetrative foliation. The large-scale F1 folds have axes that are generally perpendicular to the stretching lineation (L1). The latter is commonly associated with kinematic criteria showing top-to-SE sense of shear.

The earliest deformation D1 is locally overprinted by a second deformational event D2. These structures are associated with top-to-NW kinematic indicators and subhorizontal to gently plunging fold axes and crenulations (F2) with vergence towards the NW. Most of these structures are found close to detachment faults and are attributed to the role of detachment faulting (Rosenbaum *et al.*, 2007).

Figure 2. IMap of itinerary 1 and locations of the excursion stops. Geology is after Rosenbaum *et al.* (2007).

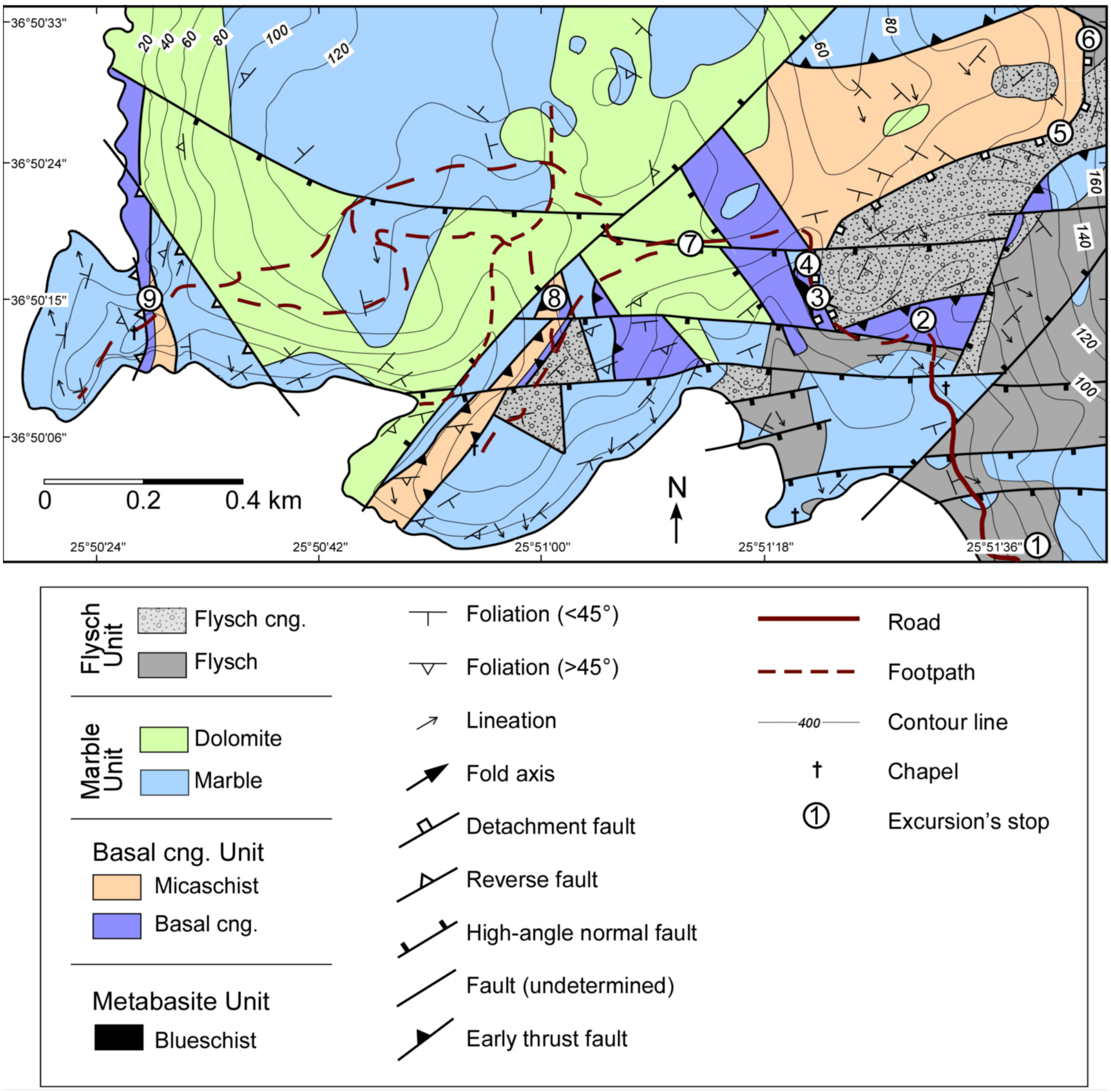

The whole sequence in Amorgos has been affected by late F3 folds. These are predominantly N-S trending folds with sub-horizontal fold axes, ranging from gently inclined tight folds to long wavelength open folds.

The actual morphology of Amorgos is largely attributed to the role of Quaternary high-angle normal faulting (Stiros *et al*., 1994). These faults are generally oriented NE-SW. One of these faults are supposedly responsible for the juxtaposition of the Pelagonian amphibolite-facies rocks of Nikouria on top of Amorgos' marble unit (Figure 1). The contact itself is not exposed.

Itinerary 1: Blueschists and carpholite-schists northwest of Katapola

The itinerary will take you through the high-pressure rocks northwest of Katapola (Figure 1), focusing on the low-angle contact between two different high-pressure units and the F3 folding of the overlying marble sequence. To reach the area, start walking along the coastline through the northern part of Katapola towards the cemetery. A map showing the itinerary and locations of the excursion stops is presented in (Figure 2).

Stop 1.1. Flysch (N 36º49'55.1", E 25º51'41.0")

Flysch is outcropping on the road from Katapola towards the cementery. The flysch consists of medium-grained sandstone and interlayered mudstone. Bedding and cleavage are developed but usually any kind of layering is highly disrupted. In this locality, the occurrence of the flysch is in the hangingwall relative to a detachment fault (see Stop 1.5).

Approximately 100 m from the cemetery, we collected a sandstone sample for fission-track dating (sample AMO 05-27). This sample contained zircon, but not apatite. It yielded an Early Cretaceous zircon fission-track age of 134±9 Ma. Another fission-track sample from the hanging wall of the Amorgos detachment was collected from flysch sandstone along the road to Chora and yielded a Late Triassic age of 219±16 Ma. Both fission-track ages are much older than the Eocene (?) depositional age of the flysch, indicating that metamorphic temperatures in the flysch were not sufficiently high to completely anneal the fission tracks in zircon. This in turn suggest that metamorphic temperatures remained below 300°C.

Stop 1.2. Conglomerate (N 36º50'14.1", E 25º51'30.3")

Continue walking on the road until it ends (near a small chapel) and becomes a footpath. Approximately 100 m after the beginning of the footpath, you will reach a gully and a small water spring. The rocks in this locality consist of strongly deformed conglomerates alternating with micaschists. They have been mapped as part of the carpholite-bearing unit (Figure 2), although they could possibly represent a sheared section of the flysch conglomerate. The conglomerate is characterised by up to 5 cm large quartz pebbles. Structures are associated with high-angle shear bands that indicate top-to-the-SE sense of movement (Figure 3), and crenulations that define an axial plane parallel to the shear bands.

Figure 3. High-angle shear bands in a conglomerate (Stop 1.1) showing top-to-the-SE sense of shear. Sample AMO 05-1 from this conglomerate yielded a zircon fission-track age of 161±15 Ma.

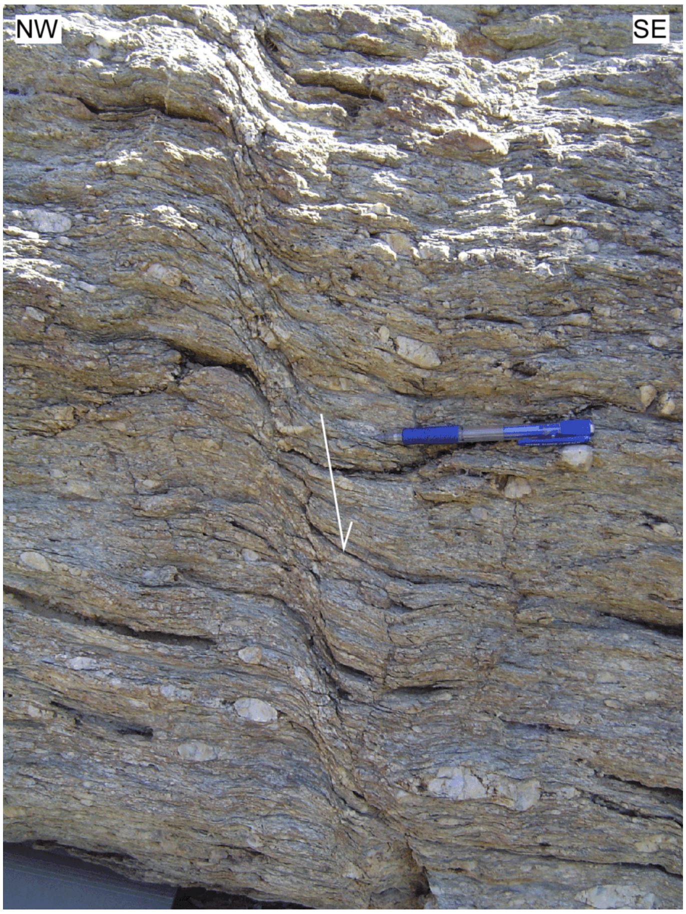

Figure 4. Metabasite blueschist-facies rock (dark green) exposed below a low-angle detachment contact (Stop 1.2).

Figure 5. Carpholite-bearing rocks from the area around Stop 1.2.

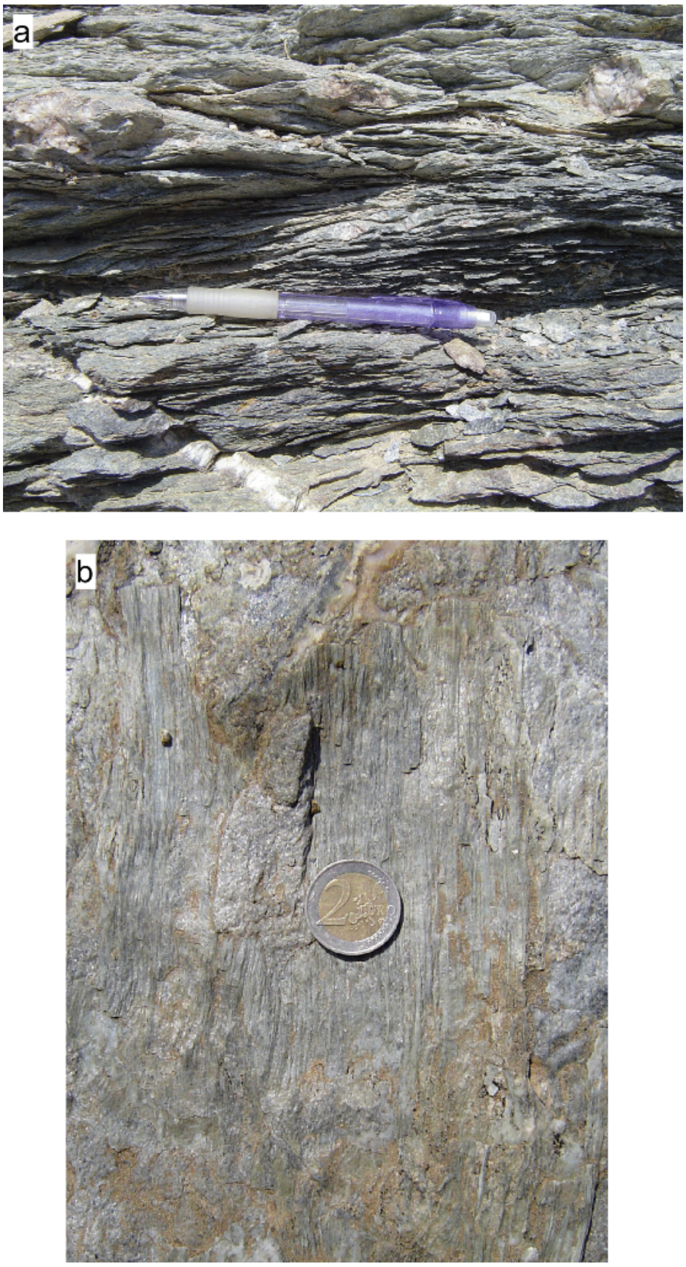

(a) Strongly sheared micaschist; (b) Stretching lineation indicated by fibrous carpholite grains.

Stop 1.3. Blueschist-facies rocks (N 36º50’18.7”, E 25º51’21.6”)

The rocks around this stop represent some of the most interesting metamorphic assemblages in Amorgos. One of these is found in a dark green metabasitic rock, which is exposed in a small outcrop on the footpath and immediately below it (Figure 4). This rock has a penetrative subhorizontal foliation on which a shallowly NW-plunging stretching lineation occur. The stretching lineation is expressed by aligned chlorite flakes and elongated albite.

Thin section examination revealed that the metabasite consists of blue-amphibole, garnet and clinopyroxene, indicating peak P-T conditions of >13 kbar and 500-600°C (Rosenbaum *et al.*, 2007). The blue amphiboles are typically magnesio-riebeckite with rims of green amphiboles (tschermakite). Garnet occurs as porphyroblasts, strongly altered to epidote and chlorite and rich in actinolite, clinopyroxene, quartz and apatite inclusions. Accessory calcite and sphene have also been recognised in thin sections. The overall preservation of the blueschist assemblage is relatively poor due to the effect of strong greenschist-facies overprint.

Metabasite sample AMO 04-16 yielded a few apatite grains, which provide an apatite fission-track age of 18.3±3.2 Ma. This age is based on only 12 dated grains but nevertheless indicates that detachment-fault-related cooling occurred in the late Early Miocene (Burdigalian).

Rocks immediately above the metabasitic block are strongly deformed schists (Figure 5a). The schists consist of quartz, phengite, paragonite and fibrous Fe-Mg-carpholite grains. The carpholite fibers are spectacular and form distinct cm- to dm-long carpholite-quartz-phengite aggregates that define a NW-trending stretching lineation (Figure 5b). Peak metamorphic conditions of 300-450°C at 10-14 kbar have been estimated for this assemblage (Rosenbaum *et al.*, 2007), indicating that this assemblage was formed in a different thermal regime compared with the adjacent blueschist-facies metabasitic rock. Therefore, the contact between the two rocks is interpreted as a tectonic contact.

The contact between the two high-pressure rocks is a strongly sheared low angle detachment fault (Figure 4). It is characterised by a 1-2 m thick zone of semi-ductile to brittle structures that grade structurally upwards into a gouge layer. A top-to-NW sense of shear is inferred based on kinematic indicators.

Stop 1.4. Carpholite-bearing meta-conglomerate (N 36º50’19.9”, E 25º51’21.2”)

Keep walking for 70-80 m up the track until reaching a platform of a meta-conglomerate rock. This rock has a purple to dark green colour, which is distinctly different from the abundant conglomerates of the flysch unit. The pebbles are derived from milky white vein quartzites, marbles and schists. Fibrous carpholite can be recognised in the matrix. Because the pebbles of the flysch conglomerates contain a much larger variety of clast lithologies, including numerous dm-large marble pebbles, we strongly believe that this conglomerate does not belong to the flysch unit.

Fission-track sample AMO 05-22 from this outcrop yielded a Middle Jurassic zircon fission-track age of 167±16 Ma, which is similar to the zircon fission-track age from the carpholite-bearing conglomerate at Stop 1.1. These older fission-track ages have nor been reset during the Tertiary orogenic history of this unit. This suggests that metamorphic temperatures remained below 300°C, thus at the very lower end of the estimated peak PT conditions reported above.

Figure 6. A strongly deformed brittle-ductile contact in Stop 1.4.

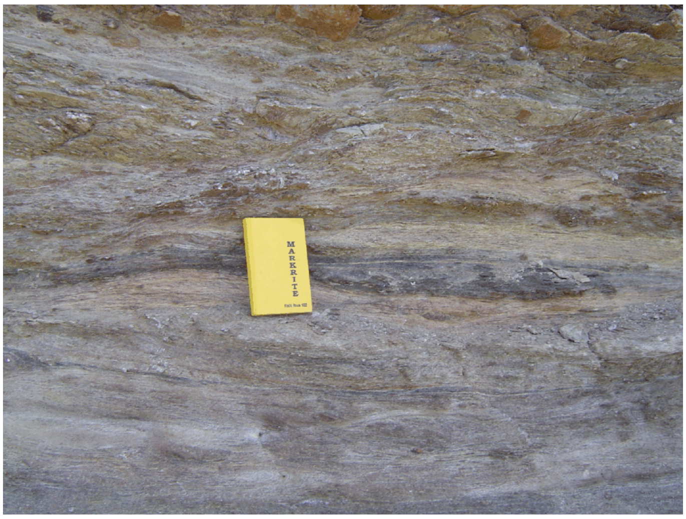

Stop 1.5. The detachment (N 36º50’26.8”, E 25º51’42.1”)

Leave the track before its sharp turn westward and walk northeastward along the contact between high-pressure albite-micaschists and flysch conglomerates. Keep walking until reaching a relatively good exposure of the detachment contact in a little rock cliff (Figure 6). The cliff consists of strongly sheared carbonate-bearing phyllites. The penetrative foliation developed under lower greenschist-facies conditions, but abundant gouge layers developing in the foliation planes attest to ongoing shear along the foliation planes in the brittle crust. There is evidence for both to top-to-the-SE and top-to-the-NW sense of movements. Based on structural evidence elsewhere in the island, it seems that the top-to-the-NW sense of shear is associated with the actual movement along the detachment, whereas the top-to-the-SE sense of shearing is inherited from an earlier deformation (Rosenbaum *et al.*, 2007).

Figure 7. Type 3 interference pattern in the flysch (Stop 1.5).

Stop 1.6. Refolded F1 folds in the flysch (N 36º50’33.2”, E 25º51’44.3”)

Approximately 200 m northward from the previous stop, you can find excellent examples of refolded structures in the flysch (Figure 7). These structures are type 3 interference patterns (Ramsay, 1967) associated with refolding of F1 isoclinal folds around F2 folds. The F2 folds are asymmetric Z shaped (down plunge) with fold hinges that shallowly plunge towards the east.

Stop 1.7 Dolomite (N 36º50’17.8”, E 25º51’05.4”)

Walk back to the curve in the main track north of stop 3, and continue westward for approximately 250 m. The rock here consists of yellow dolomite layers alternating with purple marly shales and meta-claystones (Figure 8). The meso-scale folds in the dolomite are interpreted as late F3 folds.

Figure 8. Folded dolomite and meta-claystone layers in Stop 1.6.

Stop 1.8. Albite micaschist (N 36º50’17.2”, E 25º51’00.9”)

From Stop 6, head southwestward to the crest of the peninsula. You will notice that the dip of the dominant foliation changes due to the effect of F3 folding. The foliation is nearly vertical in Stop 7, where a narrow band of albite-mica schists is exposed. This rock supposedly represents a lower structural level (part of the basal conglomerate unit) which reappears here as a result of folding and faulting. Adjacent to the micaschists, you can find a small outcrop of the meta-conglomerate with its characteristic milky white quartz veins.

Stop 1.9. Large F3 fold (N 36º50’14.6”, E 25º50’26.8”)

The last stop in this itinerary is located near the small chapel of Profitis Ilias in the westernmost part of the peninsula. In this locality, there is an excellent exposure of the fault contact between marbles in the hanging wall and micaschists and meta-conglomerates in the footwall (Figure 9a). The overlying marble is folded showing a sub-horizontal fold hinge and an axial plane that is shallowly dipping towards the east.

Figure 9. Large F3 fold in the westernmost part of the peninsula (Stop 1.8).

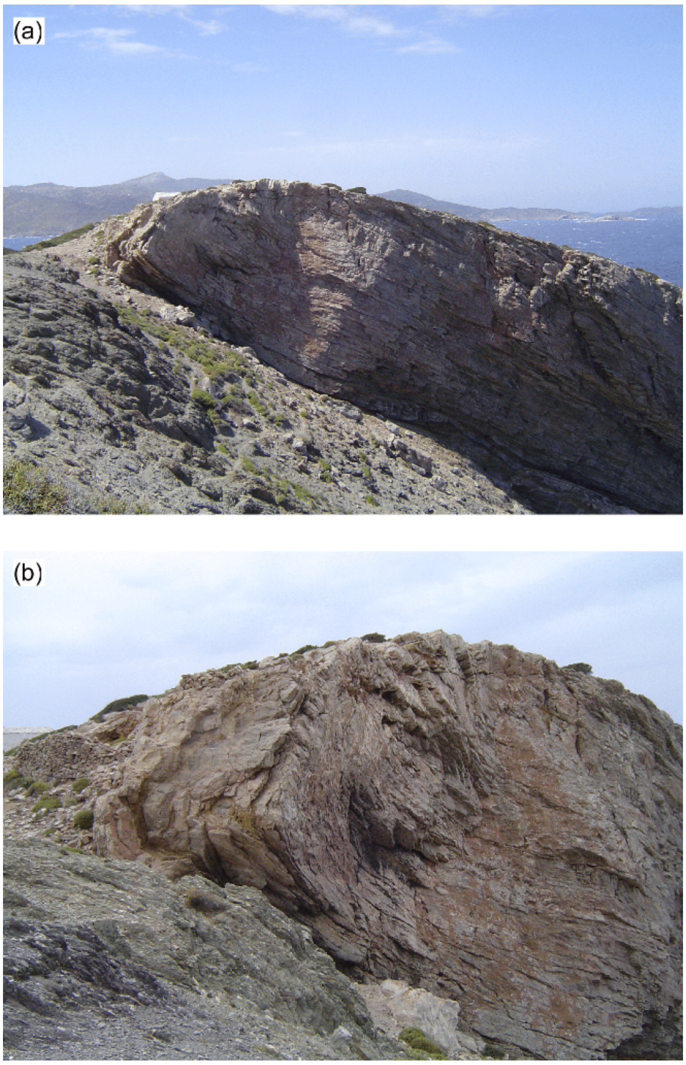

Note the excellent exposure of the fault contact between footwall schists and conglomerates and hanging wall marbles.

Itinerary 2: From Hozoviotíssas Monastery to Egiali

This itinerary is geologically more monotonous compared with the diversity of rock types in the peninsula northwest of Katapola (Itinerary 1). The rocks are predominantly marbles, with some exposures of folded flysch rocks. The structures, however, are interesting and provide information on the larger-scale folding history of Amorgos. There is a good walking path from Hozoviotíssas monastery to Egiali (Figure 10), which makes this itinerary one of Amorgos' finest walks.

Stop 2.1. Hozoviotíssas Monastery (N 36º49'56.3", E 25º54'32.9")

The monastery of Hozoviotíssas is situated on a sheer cliff 320 m above the sea level and is by far one of Amorgos' biggest highlights. It was built in the end of the 11th century and is named after the town of Hozova, from which a precious icon of the Virgin was allegedly brought by monks. The monastery is normally opened for visitors during the mornings.

From the car park, you can see a steeply dipping normal fault that separates the flysch sequence from the marble unit. The fault is characterised by numerous SE-dipping polished fault planes that have SE-plunging striations on them. Fault-slip analysis of this outcrop and a few nearby outcrops yielded a SE-directed extension direction and a subvertical shortening axis indicating normal faulting. The kinematics derived from fault slip analysis is the same as the one derived from focal-plane solutions of the 1956 MS = 7.4 earthquake. We therefore assume that the fault planes are related to coseismic uplift of Amorgos, which also appears to control the morphology of the southeastern coastline of the island.

Follow the stairs that lead to the monastery and look at the numerous fold patterns in the marble (Figure 11). The folds appear in a layered marble lithology and are sub-horizontal recumbent to gently inclined folds. Fold axes show variable orientations but their geometric distribution generally coincides with a southeast-dipping axial plane (Figure 12b). Based on overprinting relationships in Potamos (Stop 2.5), this axial plane is considered to represent a late generation of folding, i.e. F2 or F3.

Figure 10. Map of the central part of the island showing the general geology (partly after Dürr, 1985) and the locations of Itinerary 2’s excursion stops.

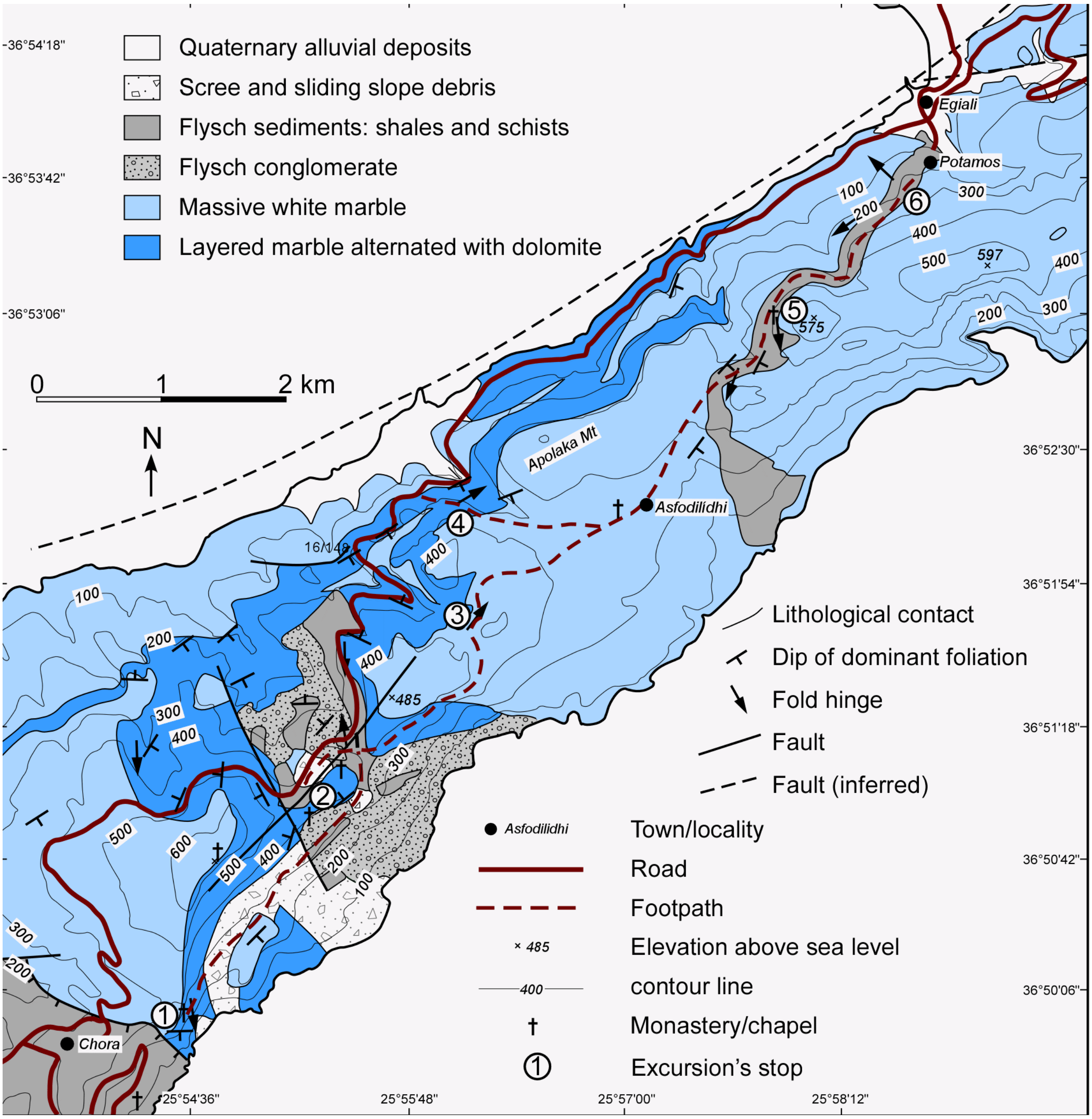

Figure 11. Fold structures in the area near the monastery of Hozoviotíssas (Stop 2.1).

(a) A sub-horizontal recumbent fold; (b) A weak development of flat lying axial plane cleavage.

Figure 12. Stops 2.5, 2.6

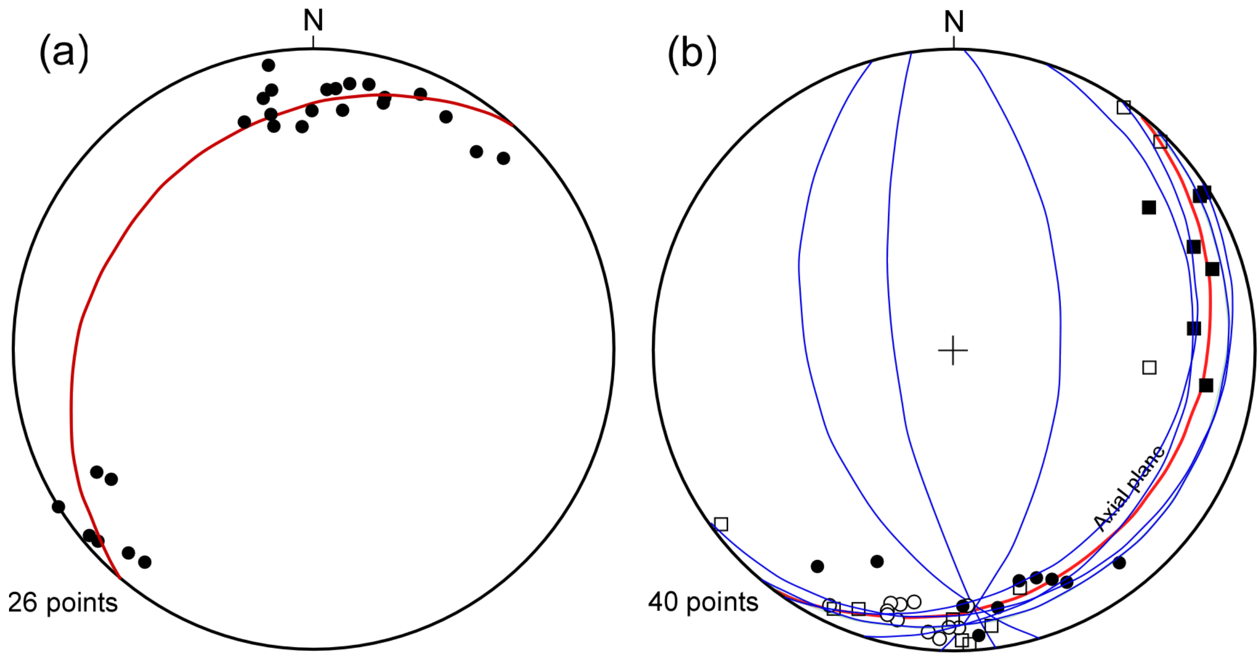

(a) F1 asymmetric folds showing geometric distribution around an axial plane (S1) that shallowly dipping towards the northwest (27º-310º). (b) F2 fold axes from Ronzas creek around Stop 2.4 (filled squares), Stops 2.5 and 2.6 (open squares), Hozoviotíssas monastery around Stop 2.1 (filled circles), and north of Hozoviotíssas monastery (open circles). The fold axes roughly coincide with a calculated S3 axial plane of 20º-127º (red girdle). The blue girdles indicate measured S1 foliations from the area around Stop 2.5.

Stop 2.2. F1 folds in the marble (N 36º51’06.8”, E 25º55’25.9”)

Take the footpath that starts at the northern gate of the monastery, and follow it northward. You will first pass scree and sliding slope debris, until reaching outcrops of deformed flysch conglomerates with kinematic indicators, such as S-C structures, that show top-to-the-SE sense of shear. The next stop is located near a small church approximately 200 meters west of the footpath.

In this area the effect of the early generation of folding (F1) is responsible for repetitions of marble, flysch and flysch conglomerate layers. One of these F1 folds is recognised in the layered marble, showing S-shaped asymmetry when looking down plunge (Figure 13). Folding is responsible for the development of the dominant shallowly dipping foliation and is recognised in a series of asymmetric folds that generally show vergence towards the SE. These fold axes roughly coincides with an axial plane (S1) that shallowly dipping towards the NW (Figure 12a). The sense of overturning, towards the SE, is therefore indicative of thrusting during D1 deformation.

Figure 13. F1 isoclinal fold in the layered marble (Stop 2.2) showing Z shaped asymmetry when observed up plunge (i.e. the fold has an S shape down plunge).

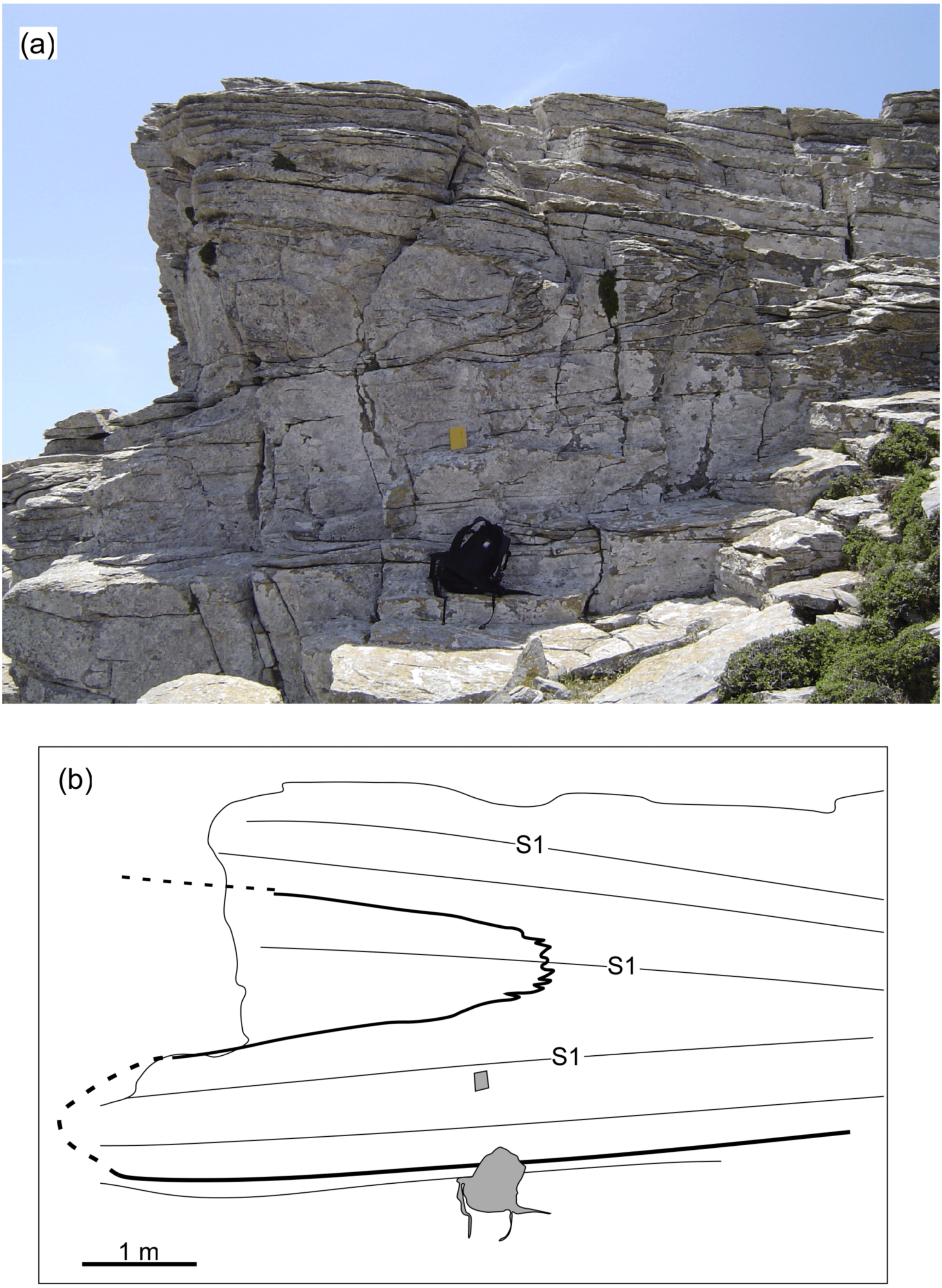

Stop 2.3. Interference patterns (N 36º51'44.5", E 25º56'08.4")

Follow the footpath that runs from the dirt road junction to the southeastern slope of hill 485 (Figure 10). Keep walking parallel to the 400 m contour until reaching the saddle between this hill and the next hill to the north.

The small outcrop in the platy marble shows interference patterns of the two generations of folding (Figure 14). The S1 fabric is folded around F2 or F3 folds, and some typical type 1 interference patterns (Ramsay, 1967) are recognised.

Figure 14. Interference patterns around Stop 2.3

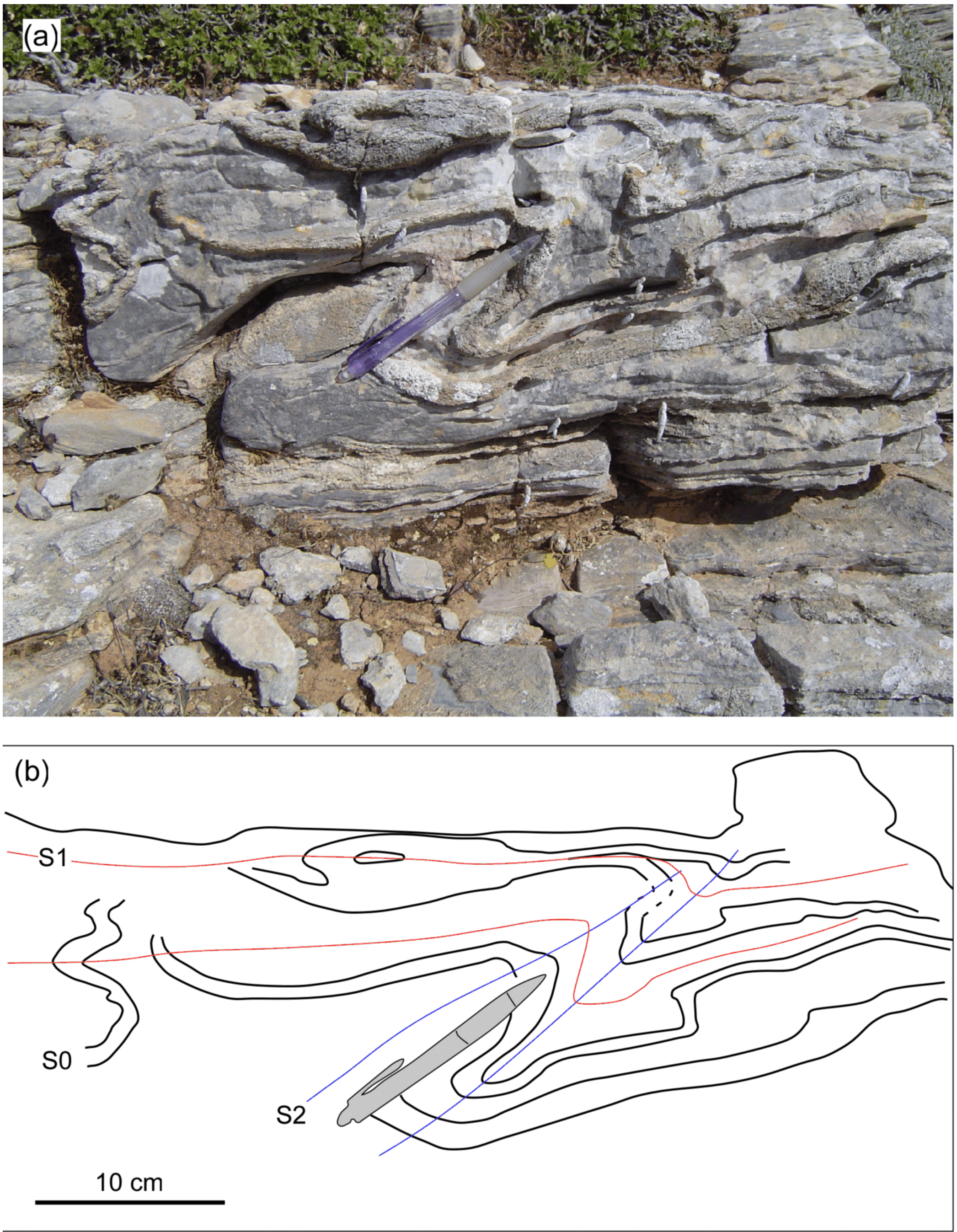

Stop 2.4. Ronzas Creek (N 36º52’13.6”, E 25º56’12.8”)

Keep walking north for approximately 1.3 km and turn left to a track that leads westward above Ronzas creek. Follow this track for another 1.2 km until reaching folds in the layered marble (Figure 15a). These fold axes mostly plunge to the NE, but like the folds in Stop 2.1, their fold orientation coincides with the second generation axial plane (Figure 12b). Looking northward over the northwestern slope of Mt Apolaka, a large-scale fold is recognised (Figure 15b).

Walking westward on the dirt road, you can see nice examples of boudinaged structures within the marble (Figure 16).

Figure 15. Folds around Ronzas creek (Stop 2.4).

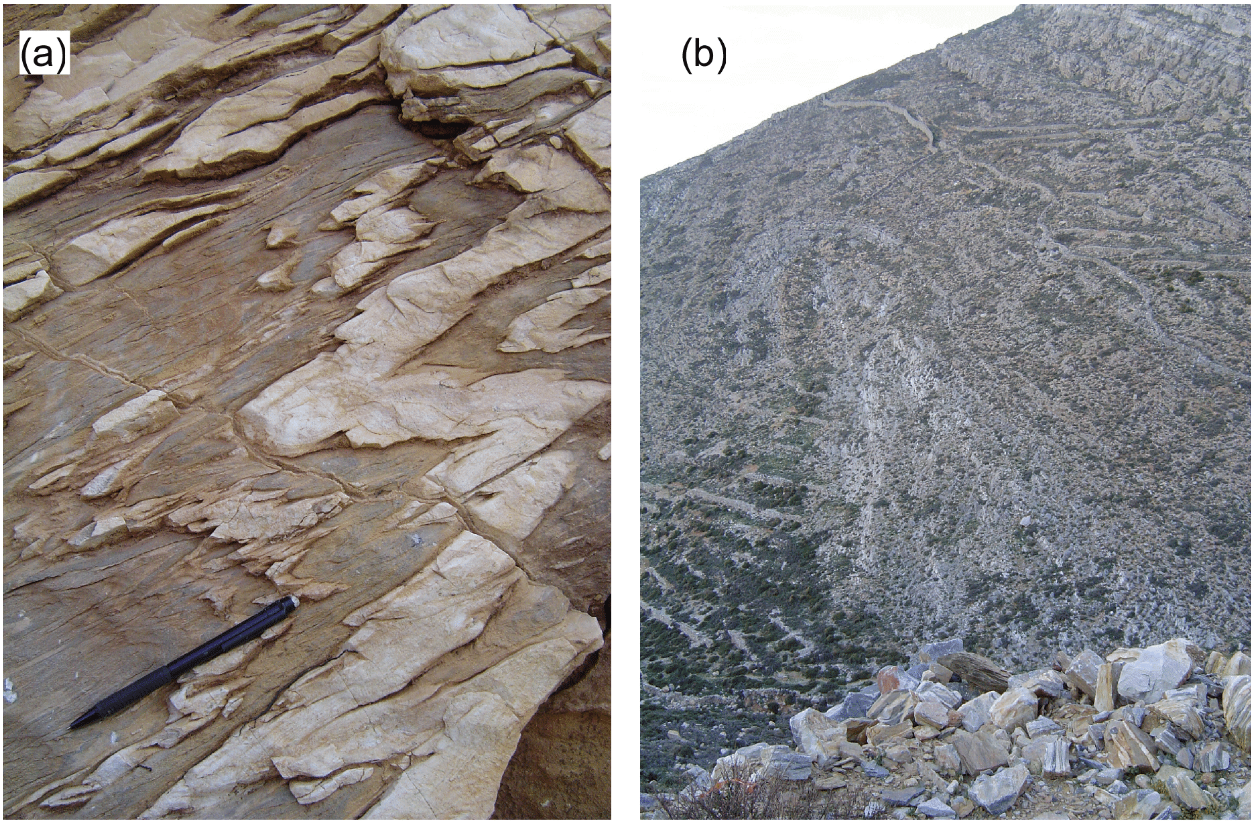

(a) Meso-scale folds in the layered marble. (b) A large scale fold at the slope of Mt Apolaka.

Figure 16. Boudinage structures in the layered marble near Ronzas creek (Stop 2.4).

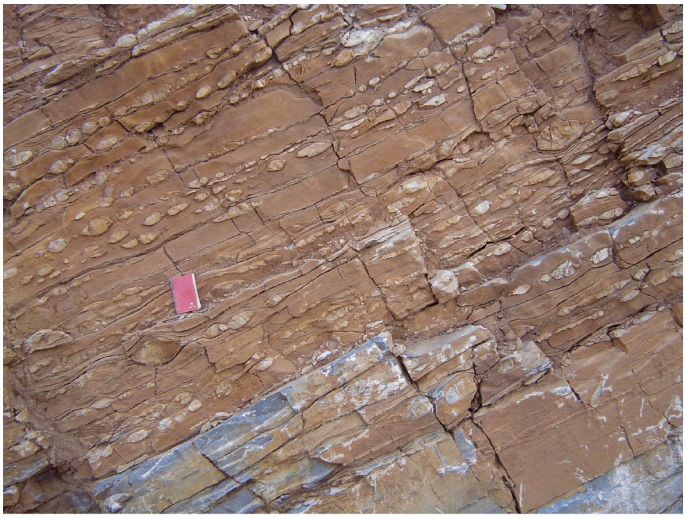

Stop 2.5. F1/F2 overprinting relationships (N 36º53’05.1”, E 25º57’47.1”)

Walk back to the footpath on the crest, and continue northwestward pass the partly inhabited village of Asfodilídhi. The track will then enter a narrow band of flysch sediments. The next stop is located above the little chapel west of hill 575.

The flysch sediments in this locality show two fabrics (Figure 17a). The earlier (S1) foliations are generally steeply dipping and show variable orientations that intersect in a ß axis of 12º-175º (Figure 12b). Folding of the S1 fabric is also recognised, forming an axial plane cleavage parallel to S2 (Figure 17b). The sense of overturning on these F2 folds is towards the northwest.

Figure 17. Overprinting relationships between S1 and S2 fabrics in Stop 2.5.

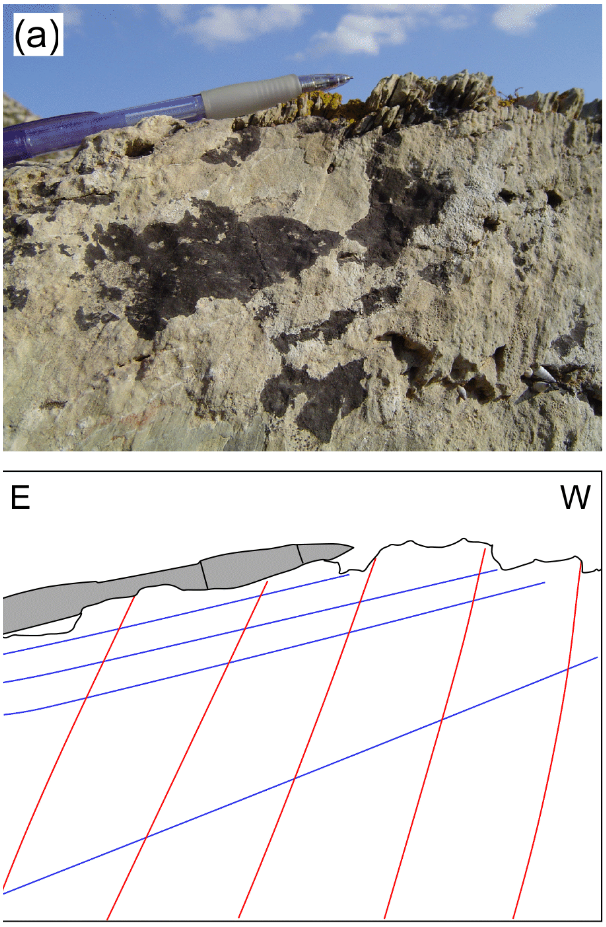

(a) Penetrative S1 foliation that steeply dipping to the east, overprinted by shallowly southeast-dipping foliation. (b) Folding of S1 and development of S2 axial plane cleavage, which is parallel to the S2 fabric shown in (a)

Stop 2.6. Potamos

As you continue walking towards the village of Potamos, you can see many F2 folds that show vergence to the NW. A similar sense of movement is also recognised by asymmetric structures in the flysch (Figure 18).

Figure 18. Top NW sense of shear indicators in the flysch around Stop 2.6

Acknowledgments

We wish to thank S. Thomson for conducting fission tracks analysis of selected samples.

References

Bernoulli, D., De Graciansky, P.C. and Monod, O., 1974. The Extension of the Lycian Nappes (SW Turkey) into the Southeastern Aegean Islands. Eclogae Geologicae Helvetiae, 67: 39-90.

Bonneau, M., 1984. Correlation of the Hellenide nappes in the south-east Aegean and their tectonic reconstruction. In: J.E. Dixon and A.H.F. Robertson (Editors), The Geological evolution of the Eastern Mediterranean. Geological Society, London, Special Publications, 17, pp. 517-527.

De Graciansky, P.C., 1972. Recherches géologiques dans le Taurus Lycien occidental. DSc Thesis, University of Paris, 571 pp.

Dürr, S., 1985. Geological Map of Greece, 1:50,000. Amorgos-Donoussa Sheet. IGME, Athens.

Dürr, S., Altherr, R., Keller, J., Okrusch, M. and Seidel, E., 1978. The median Aegean crystalline belt: stratigraphy, structure, metamorphism, magmatism. In: H. Cloos, D. Roeder and K. Schmidt (Editors), Alps, Appenines, Hellenides, 38. Scheitzerbart, Stuttgart, pp. 455-477.

Fytrolakis, N., Papanikolaou, D. and Panagopoulos, A., 1981. Stratigraphy and structure of Amorgos Island, Aegean Sea. Annales Geologiques des Pays Helleniques, 30: 455-472.

Jolivet, L., Rimmelé, G., Oberhänsli, R., Goffé, B. and Candan, O., 2004. Correlation of syn-orogenic tectonic and metamorphic events in the Cyclades, the Lycian Nappes and the Menderes massif, geodynamic implications. Bulletin de la Societe Géologique de France, 175(3): 217-238.

Minoux, L., Bonneau, M. and Kienast, J.R., 1980. L'ile d'Amorgos, une fenetre des zones externes au coeur de l'Epee (Grece), metamorphisee dans le facies schistes bleus. Comptes Rendus de l'Academie des Sciences, 291(9): 745-748.

Papadopoulos, G.A. and Pavlides, S.B., 1992. The large 1956 earthquake in the south Aegean: macroseismic field configuration, faulting, and neotectonics of Amorgos Island. Earth and Planetary Science Letters, 113: 383-396.

Perissoratis, C. and Papadopoulos, G., 1999. Sediment instability and slumping in the southern Aegean Sea and the case history of the 1956 tsunami. Marine Geology, 161: 287-305.

Ramsay, J.G., 1967. Folding and fracturing of rocks. McGraw Hill, New York, 568 pp.

Renz, C., 1933. Beiträge zur Geologie der Kykladeninsel Amorgos. Eclogae Geologicae Helvetiae, 26(2): 131-154.

Rosenbaum, G., Ring, U. and Kühn, A., 2007. Tectono-metamorphic evolution of high-pressure rocks from the island of Amorgos (Central Aegean, Greece). Journal of the Geological Society, 164: 425-438.

Stiros, S.C., Marangou, L. and Arnold, M., 1994. Quaternary uplift and tilting of Amorgos Island (southern Aegean) and the 1956 earthquake. Earth and Planetary Science Letters, 128: 65-76.

Tataris, A., 1965. Suggestions regarding the geotectonic position of Amorgos Island. Bulletin of the Geological Society of Greece, 6: 239-247.

Theye, T., Chopin, C., Grevel, K.D. and Ockenga, E., 1997. The assemblage diaspore+quartz in metamorphic rocks; a petrological, experimental and thermodynamic study. Journal of Metamorphic Geology, 15(1): 17-28.